

Over-cooled haloes at $z \geq 10$: a route to form low-mass first stars

Joaquin Prieto^{1*}, Raul Jimenez^{2,1,3}, Licia Verde^{2,1,3}

¹*ICC, University of Barcelona (IEEC-UB), Martí i Franques 1, E08028, Barcelona, Spain*

²*ICREA*

³*Theory Group, Physics Department, CERN, CH-1211, Geneva 23, Switzerland*

27 July 2021

ABSTRACT

It has been shown by Shchekinov & Vasiliev (2006) (SV06) that HD molecules can be an important cooling agent in high redshift $z \geq 10$ haloes if they undergo mergers under specific conditions so suitable shocks are created. Here we build upon Prieto et al. (2012) who studied in detail the merger-generated shocks, and show that the conditions for HD cooling can be studied by combining these results with a suite of dark-matter only simulations. We have performed a number of dark matter only simulations from cosmological initial conditions inside boxes with sizes from 1 to 4 Mpc. We look for haloes with at least two progenitors of which at least one has mass $M \geq M_{cr}(z)$, where $M_{cr}(z)$ is the SV06 critical mass for HD over-cooling. We find that the fraction of over-cooled haloes with mass between $M_{cr}(z)$ and $10^{0.2}M_{cr}(z)$, roughly below the atomic cooling limit, can be as high as ~ 0.6 at $z \approx 10$ depending on the merger mass ratio. This fraction decreases at higher redshift reaching a value ~ 0.2 at $z \approx 15$. For higher masses, i.e. above $10^{0.2}M_{cr}(z)$ up to $10^{0.6}M_{cr}(z)$, above the atomic cooling limit, this fraction rises to values $\gtrsim 0.8$ until $z \approx 12.5$. As a consequence, a non negligible fraction of high redshift $z \gtrsim 10$ mini-haloes can drop their gas temperature to the Cosmic Microwave Background temperature limit allowing the formation of low mass stars in primordial environments.

Key words: galaxies: formation — large-scale structure of the universe — stars: formation — turbulence.

1 INTRODUCTION

In the current Λ Cold Dark Matter (ACDM) cosmological paradigm, dark matter (DM) over-densities are the building blocks of cosmic structures. These DM over-densities grow due to gravity forming DM haloes in a hierarchical way, i.e. from the smaller to the bigger ones, and mergers play an important role in this process.

For the formation of the first luminous objects to become possible, the baryonic content of the haloes must be able to cool. Cooling of primordial gas is driven by molecular Hydrogen (H_2) which can form inside DM mini-haloes of mass $\gtrsim 10^6 M_\odot$. Once H_2 formation is triggered, rovibrational transitions of the H_2 molecule are able to cool the primordial gas down to temperatures of ~ 200 K (Haiman et al. 1996; Tegmark et al. 1997; Abel et al. 2002), see also the Barkana & Loeb (2001) review. At lower temperatures, the H_2 lines become insufficient to cool the gas further.

The H_2 cooling temperature floor ($T \approx 200$ K) and its

saturation number density ($n \approx 10^4 \text{cm}^{-3}$ i.e. the density for Local Thermal Equilibrium at which H_2 cooling is inefficient) yield a Jeans mass:

$$M_J \approx 500 M_\odot \left(\frac{T}{200\text{K}} \right)^{3/2} \left(\frac{10^4 \text{cm}^{-3}}{n} \right)^{1/2}. \quad (1)$$

This sets a mass scale for gravitationally bounded objects in the primordial gas, suggesting that the first stars were massive¹.

However, if the HD molecule is formed in a significant amount in primordial environments, although it has no relevant role in the first stage of H_2 driven cooling (Lepp & Shull 1983; Bromm et al. 2002) it could eventually ($T \lesssim 150$ K) become important (Bougleoux & Galli 1997; Machida et al. 2005), allowing the gas to reach temperatures as low as the Cosmic Microwave Background (CMB) temperature limit at the corresponding redshift. If HD cooling could be trig-

¹ But see Greif et al. (2011) and Stacy & Bromm (2013b) for lower masses primordial stellar binary-multiple systems.

* email:joaquin.prieto.brito@gmail.com

Table 1. Simulation parameters. We have adopted $h = 0.719$ thus lengths are in Mpc and masses in M_\odot .

| Sim. Name | Number of sims. N | Box size $L_{\text{box}}/\text{Mpc}$ | Part. number N_p | Part. mass m_p/M_\odot | $M_{cr}(z=10)/m_p$ $N_{p,h}$ | $M_{cr,1}(z=17.5)/m_p$ $N_{p,h}$ |
|-----------|------------------------|---|-----------------------|-----------------------------|---------------------------------|-------------------------------------|
| S1Mpc256 | 20 | 1 | 256^3 | 5.88×10^3 | 3.72×10^3 | 1.31×10^3 |
| S2Mpc256 | 20 | 2 | 256^3 | 4.70×10^4 | 4.66×10^2 | 1.64×10^2 |
| S4Mpc256 | 20 | 4 | 256^3 | 3.77×10^5 | 5.80×10^1 | 2.10×10^1 |
| S1Mpc512 | 5 | 1 | 512^3 | 7.35×10^2 | 2.98×10^4 | 1.05×10^4 |
| S2Mpc512 | 5 | 2 | 512^3 | 5.88×10^3 | 3.72×10^3 | 1.31×10^3 |
| S4Mpc512 | 5 | 4 | 512^3 | 4.70×10^4 | 4.66×10^2 | 1.64×10^2 |

gered, a lower temperature floor for the gas would decrease the Jeans mass and thus this process could favor the formation of low mass stars at high redshift.

Because the HD number density depends on the H_2 abundance through $\text{H}_2 + \text{D}^+ \rightarrow \text{HD} + \text{H}^+$ (Palla et al. 1995; Galli & Palla 2002) and the H_2 abundance depends on the free electron number density through $\text{e}^- + \text{H} \rightarrow \text{H}^- + \gamma$ followed by $\text{H}^- + \text{H} \rightarrow \text{H}_2 + \text{e}^-$ (Peebles & Dicke 1968), if the gas presents a high ionization fraction it is possible to increase the HD abundance. It has been shown that such high ionization fraction conditions are common in post-shocked gas inside DM haloes (Greif et al. 2008; Prieto et al. 2012). In fact, the DM halo growing process involves violent merger events. These mergers are able to produce strong shock waves which both compress the halo baryonic content and increase the ionization fraction. This drives an enhancement in the formation rate of HD molecules with the consequent over-cooling of the primordial gas, as shown in Greif et al. (2008) and Prieto et al. (2012).

Shchekinov & Vasiliev (2006) (hereafter SV06) studied the necessary (thermo-chemical) conditions for HD cooling to switch on. They argue that such conditions are fulfilled in merging DM haloes with a total system mass above a critical value, so suitable shocks form. The post-shocked gas with an enhanced HD molecular fraction is able to drop its temperature to the CMB floor of $T_{\text{CMB}} \approx 2.73(1+z)$.

SV06 however only considered a straw-man head-on collision of two primordial clouds of equal mass, but, clearly the physical state of the post-shock gas depends on many factors that are not captured by this simplified scenario. Prieto et al. (2012) produced numerical DM + baryons simulations that capture enough physics to study the physical state of the post-shock gas. They find that as a result of the hierarchical merging process, turbulence is generated and the production of coolants is enhanced, so much that even the HD molecule becomes an important coolant in some regions. Yet, their simulations are not sufficient to assess how generic this is, that is, how these regions are associated to the distribution of minihaloes. This is what we set up to do here.

In this paper, we use a set of DM cosmological simulations to compute the fraction of haloes able to produce over-cooling of the primordial gas due to mergers at high redshift as predicted by SV06 using the recipe developed in Prieto et al. (2012). The paper is organized as follows. In §2 we describe our methodology. In §3 we show our numerical results and discuss about them. In §4 we present our summary and conclusions.

2 METHODOLOGY

In principle, to compute the fraction of haloes able to over-cool their baryonic content due to mergers at high redshifts, we would want to have multiple hydrodynamic simulations, which model both dark matter and baryonic physics and chemo-thermal evolution of primordial gas, for cosmological initial conditions, reaching a resolution of $\sim 1\text{pc}$ at $z=10$. This ambitious goal was achieved in Prieto et al. (2012) but only for a single 1 Mpc size box and in there the formation and baryonic matter accretion process of a single halo was simulated at full resolution: a region of 2 kpc (at $z=10$) with $\sim 2\text{pc}$ resolution (at $z=10$). The average CPU-time for one of such systems is ~ 180000 CPU-hrs. This makes it computationally very expensive to replicate the Prieto et al. (2012) runs for multiple haloes in a cosmological context. However this complex problem can be broken in three ingredients which can be studied independently. The first ingredient is the thermo-chemical conditions for the HD cooling to switch on which were studied in SV06. The second ingredient is the physical conditions of the primordial gas (turbulence and shocks) which was studied in Prieto et al. (2012). They find that post shock regions are able to produce both H_2 and HD molecules very efficiently even in small mini-haloes ($M \sim 10^6 M_\odot$) if they accrete on, or merge with, a more massive but still relatively low mass halo ($M \sim 10^7 M_\odot \simeq M_{cr}$). The remaining ingredient is how frequently this happens in a cosmological context. This last step, however, can be addressed with DM-only simulations under minimal assumptions, and this is what we set up to do here.

The critical mass to trigger HD molecular over-cooling at redshift z is defined by SV06 as:

$$M_{cr}^{SV06}(z) = 8 \times 10^6 \left(\frac{20}{1+z} \right)^2 M_\odot. \quad (2)$$

Following SV06 this is the total mass of the system, i.e. DM plus baryonic mass. Because we have to work with DM only simulations, we have to make an assumption regarding the baryonic matter. To take into account the gas inside the DM haloes we assume that these primordial haloes host the universal baryon fraction

$$\frac{M_b}{M_{DM} + M_b} = \frac{\Omega_b}{\Omega_m} \equiv f_b, \quad (3)$$

where M_b , M_{DM} , Ω_b , Ω_m and f_b are the baryonic mass content of the halo, the dark mass content of the halo, the

Table 2. Relevant redshift and mass bins. The mass bins labeled by $i = 1, 2, 3$ have been chosen so that bin mass lower and upper boundaries are $10^{0.2(i-1)}M_{cr}(z_2)$ and $10^{0.2(i)}M_{cr}(z_2)$ respectively. The mass range spanned by the three bins covers the transition from H_2 cooling haloes to atomic cooling ones.

| z_1 | z_2 | Mass bin 1 in $10^7 M_\odot$ | Mass bin 2 in $10^7 M_\odot$ | Mass bin 3 in $10^7 M_\odot$ |
|-------|-------|---------------------------------|---------------------------------|---------------------------------|
| 10.0 | 10.2 | 2.10 - 3.33 | 3.33 - 5.28 | 5.28 - 8.36 |
| 11.0 | 11.4 | 1.73 - 2.74 | 2.74 - 4.34 | 4.34 - 6.88 |
| 12.3 | 12.7 | 1.41 - 1.81 | 1.81 - 2.87 | 2.87 - 4.55 |
| 14.9 | 15.4 | 0.99 - 1.57 | 1.57 - 2.49 | 2.49 - 3.94 |
| 17.2 | 17.9 | 0.74 - 1.17 | 1.17 - 1.85 | 1.85 - 2.94 |

Table 3. Total number of OC haloes (i.e. the sum over the N realizations) and total number of haloes (N_h) in a given mass bin with $f_{mg} = 0.6$ and $m_p \leq 5.88 \times 10^3 M_\odot$ at $z_1 = 10$.

| Sim. Name | Mass bin 1 $N_{OC}(N_h)$ | Mass bin 2 $N_{OC}(N_h)$ | Mass bin 3 $N_{OC}(N_h)$ | Total Volume Mpc^3 |
|-----------|--------------------------------|--------------------------------|--------------------------------|----------------------------|
| S1Mpc512 | 5 (7) | 4 (4) | 3 (3) | 5 |
| S1Mpc256 | 25 (46) | 14 (15) | 11 (12) | 20 |
| S2Mpc512 | 88 (132) | 56 (57) | 37 (38) | 40 |

current average baryonic matter density in the Universe in units of the critical density, the current average DM density in the Universe in units of the critical density and the universal baryonic mass fraction of the Universe, respectively. Using this approximation, the necessary (but not yet sufficient) condition for a DM halo at redshift z to become an over-cooled halo is that it must have a DM mass above a critical mass

$$M_{cr}^{DM}(z) = (1 - f_B) \times M_{cr}^{SV06}(z), \quad (4)$$

hereafter we will refer to M_{cr}^{DM} as M_{cr} .

We use the cosmological hydrodynamical code **RAMSES** (Teyssier 2002) to perform 75 DM-only simulations. The cosmological initial conditions are produced with the **mpgrafic** code (Prunet et al. 2008) and the initial redshift for each run is set to $z_i \approx 65$. The cosmological parameters are those of the concordance Λ CDM model from Komatsu et al. (2009, 2010): $\Omega_m = 0.258$, $\Omega_\Lambda = 0.742$ $h = 0.719$, $\sigma_8 = 0.796$, $n_s = 0.963$ and the transfer function of Eisenstein & Hu (1998) with $\Omega_b = 0.0441$.

Using the **AHF** halo finder (Knollmann & Knebe 2009), we identified DM haloes (i.e., objects with a density contrast $\delta \geq 200$) with mass above or equal to the critical mass to enhance the HD molecular cooling M_{cr} , at several redshifts $z \geq 10$. For reference, in the cosmology adopted here, $f_b = 0.1709$, and thus

$$M_{cr}(z) = 6.63 \times 10^6 \left(\frac{20}{1+z} \right)^2 M_\odot. \quad (5)$$

In the set-up chosen for the **AHF** halo finder the minimum particle number per halo was set to $N_{min} = 20$. We adopted this low number because we are not interested in character-

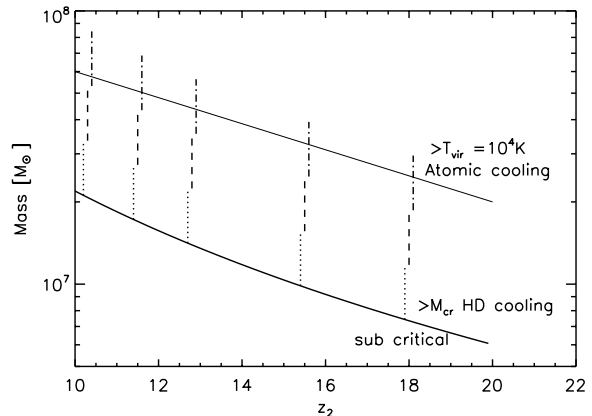


Figure 1. The mass scales involved. The lower solid line shows the critical mass for HD cooling $M_{cr}(z)$, the upper solid line corresponds to $T_{vir} = 10^4 K$ necessary for atomic lines cooling. The vertical bars (dotted, dashed and dot-dashed) correspond to the three mass bins considered.

izing the haloes based on their internal-radial features. This corresponds closely to the minimum number of particles per critical mass halo $N_{p,h}$ at the highest redshift of interest in the lower resolution run.

Table 1 shows the details of each simulation. From the first column to the last one: the simulation name, referring to both the box size and the particle number, the number of simulations N , the box size² L_{box} in Mpc, the number of particles per simulation N_p , the particle mass m_p and the number of particle per critical mass halo $N_{p,h}$ at two reference redshift $z = 10$ and $z = 17.5$.

As we will show in the next section, the most reliable results come from runs where M_{cr} is defined by $N_{p,h} \geq 1310$ particles at $z \leq 17.5$, i.e. runs with a particle mass $m_p \leq 5.88 \times 10^3 M_\odot$. In these runs the DM haloes are found consistently in successive snapshots. Furthermore, it is worthwhile to note that in these reliable runs the primordial perturbation distance scale $\lambda_{M_{cr}}$ associated to the critical mass M_{cr} is well defined by a number of particles (> 10) when the simulation start.

The Prieto et al. (2012) findings indicate that a necessary and sufficient condition for triggering HD cooling is that a halo with mass greater than M_{cr} (recall that at the redshifts of interest $M_{cr} \sim 10^7 M_\odot$) undergoes a merger or accretes baryonic material funnelled in the halo along filaments. Even in sub-critical haloes ($M \sim 10^6 M_\odot$) HD cooling can be triggered if they accrete on a critical one, as the relevant physical condition driving the turbulence is the relative velocity, which is set by the potential well created by the super-critical halo. In the super-critical halo, if it is not disrupted by a major merger, the turbulence triggered by accretion is enough enhance the creation of H_2 and HD and therefore kickstart over-cooling.

Informed by the above findings, here we impose the conditions for over-cooling to happen as follows.

We construct the merger trees for each simulation using

² Note that we adopt the value $h = 0.719$ therefore here length are in Mpc and masses in M_\odot .

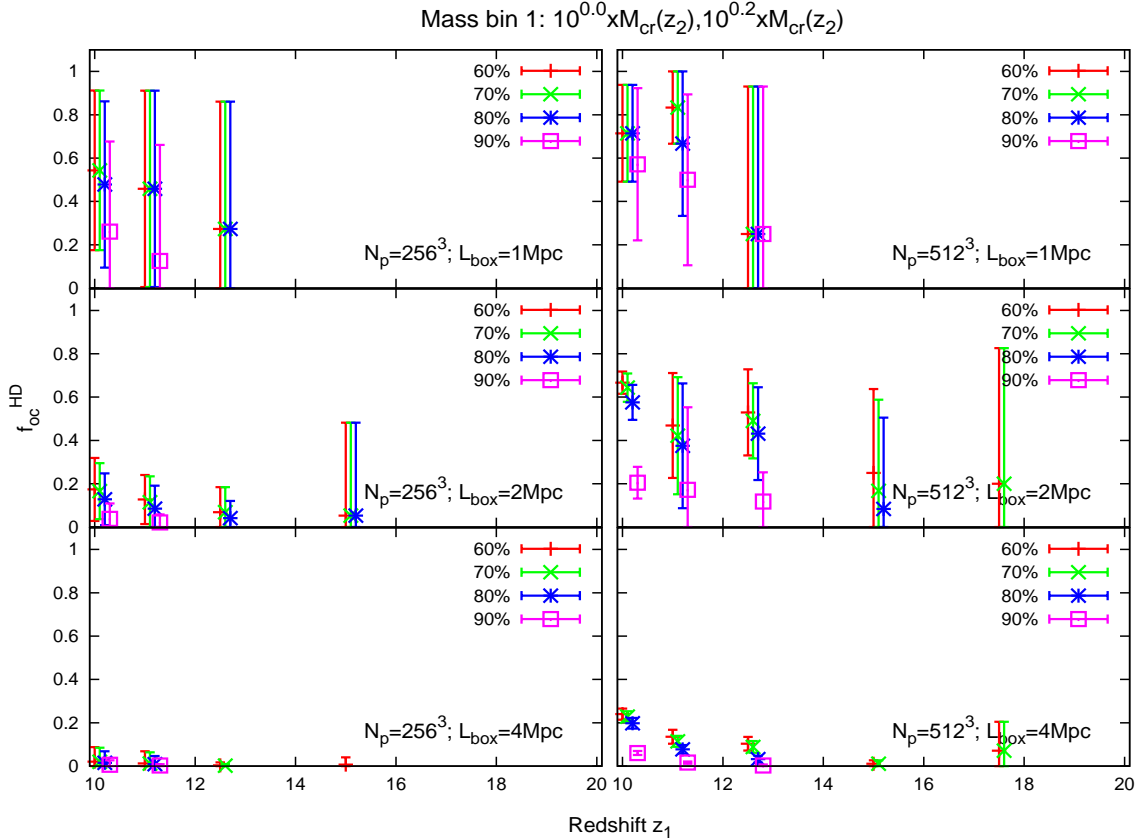


Figure 2. Fraction of over-cooled haloes $f_{\text{OC}}^{\text{HD}}$ in the first mass bin centered around $M = 1.3M_{\text{cr}}(z_2)$ (see table 2) for different merger parameters $f_{\text{mg}}=0.6, 0.7, 0.8$ and 0.9 , indicated by plus, 'x', stars and square symbols respectively. The results are shown for each redshift z_1 from table 2: $z_1 = 10.0, 11.0, 12.3, 14.9$ and 17.2 . The left column shows the low resolution runs with 256^3 particles and the right column shows the high resolution runs with 512^3 particles. The upper row shows the 1Mpc runs, the middle row shows the 2Mpc runs and the bottom row shows the 4Mpc runs. The high-resolution, numerically converged set-up corresponds to the top two panels and the middle row right panel.

the AHF merger tree tool, we identify DM haloes at redshift z_2 with mass $\geq M_{\text{cr}}(z_2)$ that subsequently undergo merging to form a bigger halo at z_1 (with $z_2 \geq z_1$).

We define the over-cooled (OC) halo merger as the process in which an existing halo at z_1 has at least two progenitors, of which at least one with mass $M_{\text{DM}} \geq M_{\text{cr}}(z_2)$ and after the merger keeps at least a mass fraction f_{mg} of the most massive progenitor. We vary the factor f_{mg} from 0.6 to 0.9 in order to study how the OC haloes fraction depends on it.

Our parameters of the halo finder routine imply that the minimum halo mass (which sets therefore the definition of merger) is somewhat resolution-dependent ranging from $1.47 \times 10^4 M_{\odot}$ in simulation S1Mpc512 to 7.54×10^6 in simulation S4Mpc256.

Here we want to stress that we do not impose a minimum merger mass ratio in our strategy to look for OC haloes. The method described above is suitable to address the question: *what is the fraction of DM haloes able to over-cool their baryonic content (and thus potential site for low mass star formation) due to mergers and accretion at high redshift?* Indeed, the condition $M \geq M_{\text{cr}}$ ensures that the interaction between haloes will be strong enough to trigger

the enhancement of the HD formation. On the other hand, a study based on the merger mass ratio could give us information about the amount of OC gas and then could help answer a different question: *what is the amount of OC gas in haloes at high redshift?* Our simulation set up and our methodology cannot quantify the amount of over-cooled gas but it is suitable to estimate the fraction of OC haloes at high redshift. This is the goal of the present work.

3 RESULTS AND DISCUSSION

Table 2 shows some example combinations of redshifts z_1 and z_2 used in building our merger tree, and the ranges of the three halo mass bins (at z_2) we consider. The mass bins labeled by $i = 1, 2, 3$ have been chosen so that bin mass lower and upper boundaries are $10^{0.2(i-1)} M_{\text{cr}}(z_2)$ and $10^{0.2(i)} M_{\text{cr}}(z_2)$ respectively. Thus the three mass bins are centered around, 1.3, 2.0, and 3.2 $M_{\text{cr}}(z_2)$, respectively. With this choice, the mass range spanned by the three bins covers the transition from H_2 cooling mini-haloes (with virial temperature $T_{\text{vir}} \lesssim \text{few} \times 10^3 \text{K}$ and $M_{\text{vir}} \lesssim 1.5 \times 10^7 M_{\odot}$) to

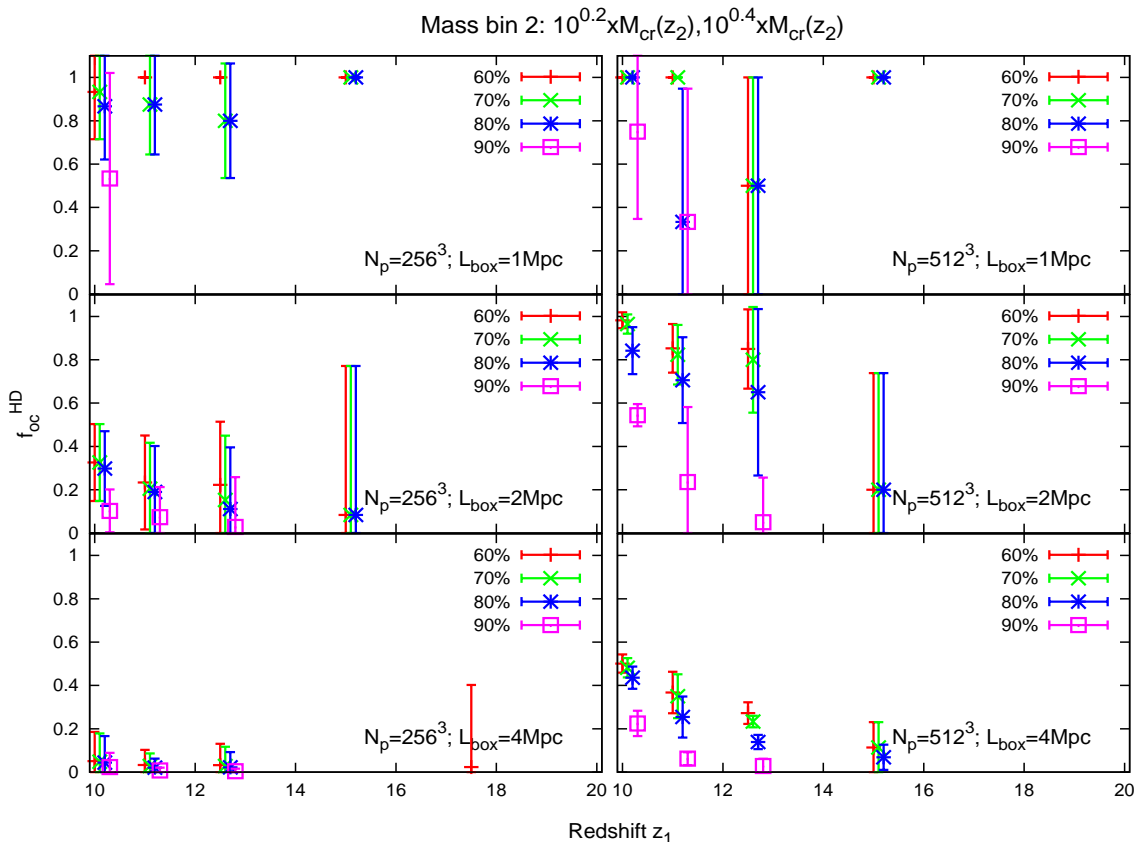


Figure 3. Same as figure 2 but for the second mass bin centered around $M = 2M_{cr}(z_2)$. See table 2.

atomic cooling haloes (with $T_{vir} \gtrsim \times 10^4$ K and $M_{vir} \gtrsim 1.5 \times 10^7 M_\odot$). This is summarized in Fig. 1.

Table 3 reports the total number of OC haloes N_{OC} and the total number of haloes N_h at $z_1 = 10$ for the three different mass bins in the less restrictive case $f_{mg} = 0.6$ and for the highest resolution simulations with $m_p \leq 5.88 \times 10^3 M_\odot$. The reported number is the sum of all OC haloes (all haloes) in the N simulations considered, i.e., 5 simulations of S1Mpc512, 20 for S1Mpc256 and 5 for S2Mpc512. The effective volume for finding these OC haloes is therefore 5 Mpc^3 , 20 Mpc^3 and 40 Mpc^3 , respectively.

Figures 2, 3 and 4 show the fraction of OC haloes f_{OC}^{HD} for four different values of f_{mg} and for the three halo mass bins as a function of redshift. These results are shown for our two different N_p (in different columns) and different box sizes L_{box} (in different rows). The error bars correspond to the standard deviation between the N simulations at a given redshift. The error on the mean would be smaller by a factor \sqrt{N} .

As we expected, the higher the f_{mg} the lower the OC fraction f_{OC}^{HD} . This trend shows that after a merger process it is very difficult for the resulting halo to keep 100% of its progenitor’s mass: some of the progenitor’s mass is always removed from the parent halo after the merger. The resulting f_{OC}^{HD} shows a very weak dependence (or no dependence at all) on f_{mg} for $0.6 \leq f_{mg} \leq 0.8$.

Our results show a clear resolution dependence for

$m_p \geq 4.70 \times 10^4 M_\odot$, i.e. runs S4Mpc512, S4Mpc256 and S2Mpc256. In these runs it is possible to see a monotonic growth of the OC fraction with the simulation resolution, which is particularly marked in the $f_{mg} = 0.6$ case: we thus discuss numerical convergence before further interpreting Figs. 2, 3 and 4.

Numerical convergence is investigated further in Fig. 5 where it is possible to identify a mass-resolution dependent trend. Simulations S1Mpc512, S2Mpc512 (and S1Mpc256) have particle masses below $m_p = 5.88 \times 10^3 M_\odot$ and thus a mass threshold for OC halo merger $M = 1.2 \times 10^5$ ($M = 1.47 \times 10^4$) or mass merger ratios below 1 : 65. These simulations correspond to the (red) plus symbols, (blue) asterisk symbols and (green) “x” symbols. At this resolution results for f_{OC}^{HD} appear to converge. On the other hand simulations S2Mpc256, S4Mpc512 and S4Mpc256 with $m_p \geq 4.70 \times 10^4 M_\odot$, (magenta) open square symbols, (cyan) filled square symbols and (yellow) open circle symbols, do not show numerical convergence. This can be understood as the mass threshold for merger in these simulations is high ($> 9.4 \times 10^5 M_\odot$) and the merger mass ratios are larger than 1 : 2.

In what follows we will focus on these three higher mass resolution simulations because they have the most reliable results based on both, convergence and number of particles per DM halo.

In figure 2, corresponding to the first mass bin (see table

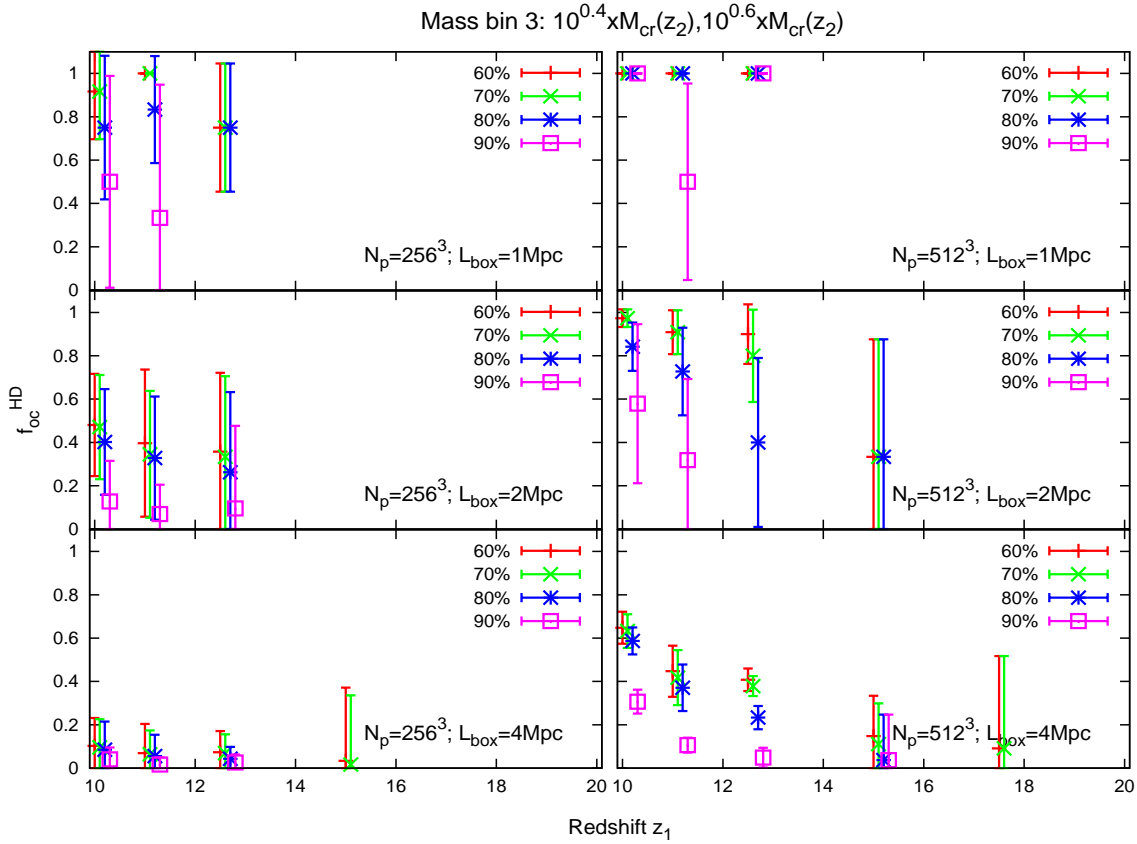


Figure 4. Same as figure 2 but for the third mass bin centered around $M = 3.2M_{cr}(z_2)$. See table 2.

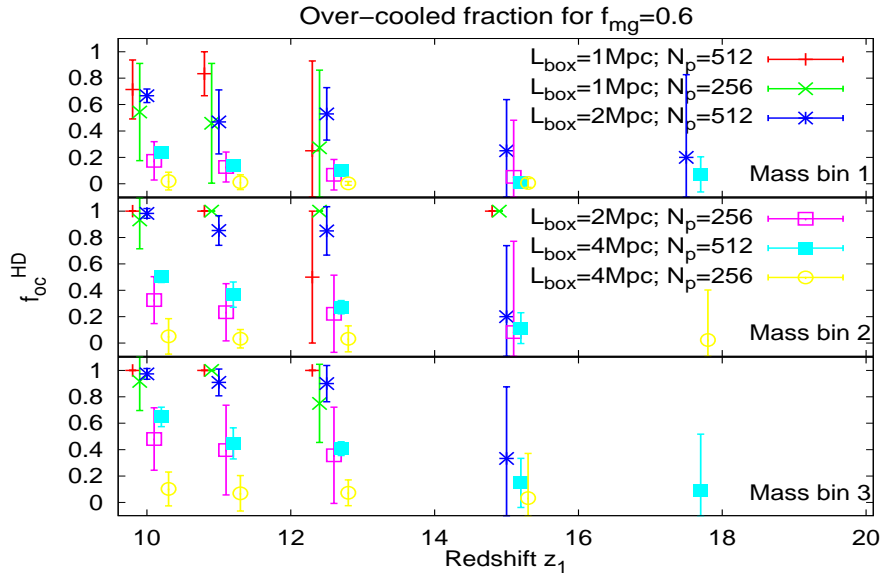


Figure 5. Over-cooled fraction for the less restrictive case $f_{mg} = 0.6$ as a function of redshift. Different symbols correspond to our six different simulations: (red) "plus" symbol for S1Mpc512, (green) "x" symbols for S1Mpc256, (blue) asterisks for S2Mpc512, (magenta) empty squares for S2Mpc256, (cyan) filled squares for S4Mpc512 and (yellow) circles for S4Mpc256. A mass-resolution dependent trend appears: S1Mpc512, S1Mpc256 and S2Mpc512 with $m_p \leq 5.88 \times 10^3 M_\odot$ have consistent f_{OC}^{HD} . S2Mpc256, S4Mpc512 and S4Mpc256 with $m_p \geq 4.70 \times 10^4 M_\odot$ have resolution-dependent f_{OC}^{HD} with is lower but increases with resolution.

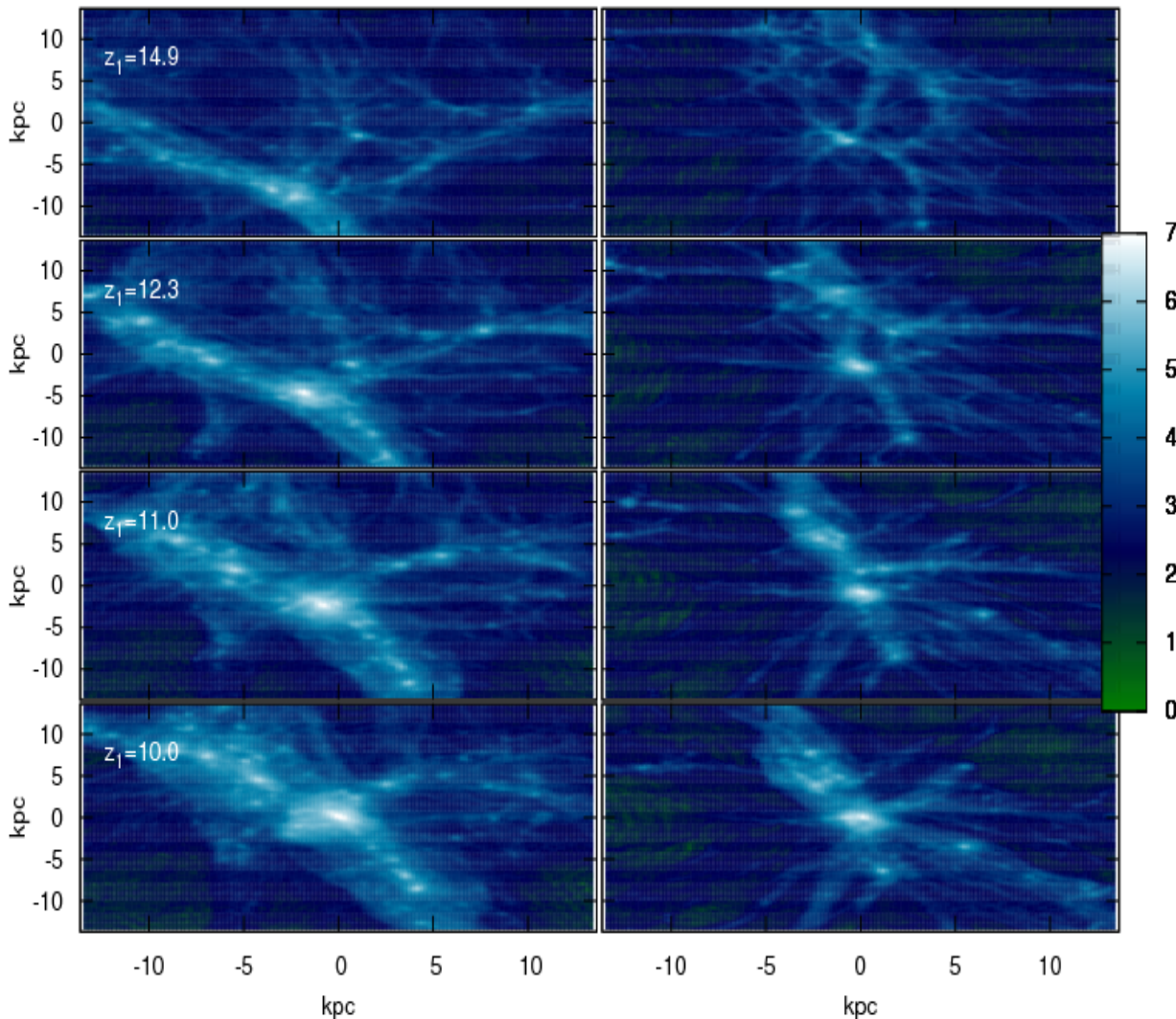


Figure 6. Dark matter mass projection in arbitrary units for two randomly chosen OC haloes. The halo on the left belongs to mass bin 3 ($M = 6.41 \times 10^7 M_\odot$ at $z = 10$) and the halo on the right to mass bin 1 ($M = 2.53 \times 10^7 M_\odot$ at $z = 10$). Each row corresponds to a different redshift z_1 . The distance scales are in co-moving kpc.

2), and for mass resolution $m_p \leq 5.88 \times 10^3 M_\odot$ (i.e., top two panels, and middle right panel) our results show that at $z = 10$ the fraction of OC haloes is $f_{\text{OC}}^{\text{HD}} \gtrsim 0.5$ in the case with $f_{\text{mg}} \lesssim 0.7$. This fraction tends to decrease at higher redshift ($z \lesssim 12.5$) but is always above 20% (for $f_{\text{mg}} \lesssim 0.7$) showing that a non negligible fraction of DM haloes in this mass bin is able to over-cool their gas content due to mergers at high redshift. At higher redshifts, i.e., $z \gtrsim 15$, the fraction decreases $f_{\text{OC}}^{\text{HD}} \lesssim 0.2$. This last result comes from S2Mpc512, the only simulation with data above $z \gtrsim 15$ in this mass bin.

In figure 3 we show the second mass bin centered around $M = 2M_{\text{cr}}(z_2)$. For runs with mass resolution $m_p \leq 5.88 \times 10^3 M_\odot$ (top two panels, and middle right panel) the OC fraction at $z = 10$ is $f_{\text{OC}}^{\text{HD}} \gtrsim 0.9$ for $f_{\text{mg}} \lesssim 0.7$ and it can reach $f_{\text{OC}}^{\text{HD}} \sim 1.0$. At higher redshift ($z \lesssim 12.5$) the fraction

remains significant, $f_{\text{OC}}^{\text{HD}} \gtrsim 0.8$. As expected the OC fraction increases with the mass of the halo.

Figure 4 shows our results for the third mass bin centered around $M = 3.2M_{\text{cr}}(z_2)$. The OC fraction keeps increasing with halo mass.

In summary these figures show that a non negligible fraction of DM haloes above the critical mass M_{cr} are able to over-cool their gas content due to mergers at high redshift.

To illustrate how the OC merger proceeds, figure 6 shows the evolution of two randomly chosen OC haloes from our catalog at 4 different redshift z_1 . In the first column we show an OC halo of $M = 6.41 \times 10^7 M_\odot$ (computed at $z = 10$) from the third bin mass and in the second column a $M = 2.53 \times 10^7 M_\odot$ (computed at $z = 10$) OC halo from the

first mass bin. The difference in size of the objects reflects the different mass bins.

As an additional study, we have computed the probability distribution function for the halo spin parameter λ defined by Bullock et al. (2001a) and we have found that it follows log-normal distribution characterized by a standard deviation $\sigma \approx 0.5$ and an average spin parameter $\bar{\lambda} \approx 0.04$ in good agreement with previous works, e.g. Davis & Natarajan (2009). Despite of the low number of haloes in the most reliable runs (see table 3), we recover a log-normal distribution (for S1Mpc256 and S2Mpc512) characterized with the parameters shown above. This fact supports our claim on the reliability of our results.

While the N-body simulations for this work were running, new results on cosmological parameters, derived from the *Planck* satellite observations, were released (Planck Collaboration 2013). The *Planck*'s best fit Λ CDM cosmological parameters are somewhat different from WMAP's ones. Because our results can be cosmology-dependent, let us elaborate on the possible effect of the *Planck* results. *Planck*'s Ω_m value is slightly higher than WMAP's and Ω_b slightly lower. This affects directly the computation of the DM critical mass $M_{cr}(z)$ decreasing it by a 2%, approximately. Furthermore, because the *Planck*'s value of the Hubble constant is lower, each redshift in our calculations has to be increased by about 4% and so the box size L_{box} . Thus the changes associated to the new best fit cosmological parameters have a negligible effect on our results.

4 SUMMARY AND CONCLUSIONS

We have performed 75 DM-only cosmological simulations with two different particle numbers (256^3 and 512^3) and inside three different box sizes ($L_{\text{box}} = 1\text{Mpc}$, 2Mpc and 4Mpc) in order to quantify the fraction of haloes able to over-cool their baryonic content due to mergers at high redshift as predicted by Shchekinov & Vasiliev (2006).

As shown in Prieto et al. (2012) accretion and (minor) mergers onto a halo of mass above the critical value defined by SV06, $M_{cr}(z)$ produce supersonic turbulence and a shocked environment where H_2 and HD molecules are formed efficiently. There, regions are able to (over)cool below the H_2 cooling temperature floor.

To identify the fraction of haloes where the above conditions are verified, we computed the progenitor's mass for each halo at a given redshift inside a bin mass, specified in table 2. This mass range spans the transition between H_2 molecular cooling to atomic cooling haloes. Every halo with more than one progenitor of which at least one has a mass above $M_{cr}(z)$, was counted as an over-cooled (OC) halo.

Our results show that a non negligible fraction of the mini-haloes formed at $z \geq 10$ over-cooled their primordial gas due to the process outlined above. The fraction of OC haloes at $z = 10$ is $f_{\text{OC}}^{\text{HD}} \gtrsim 0.5$ for masses roughly below the atomic cooling limit: $1 \times 10^7 \lesssim M/M_{\odot} \lesssim 3 \times 10^7$. At higher redshift, $z \lesssim 12.5$, the fraction $f_{\text{OC}}^{\text{HD}} \gtrsim 0.2$ and it is below 0.2 for $z \gtrsim 15$. The fraction of OC haloes rises with halo mass. For haloes above the atomic cooling limit, $2 \times 10^7 \lesssim M/M_{\odot} \lesssim 8 \times 10^7$, the fraction of OC haloes at $z \lesssim 12.5$ is $f_{\text{OC}}^{\text{HD}} \gtrsim 0.8$.

The existence of a non negligible fraction of OC haloes

at high redshift has interesting consequences for the star formation process in primordial environments. As predicted by SV06 the HD molecular cooling drops the gas temperature to the CMB limit $T_{\text{CMB}}(z) \approx 2.73(1+z)$ allowing the formation of low mass primordial stars (Prieto et al. 2011, 2012). Their low mass makes these primordial (population III) stars very long-lived opening a window for the potential detection of primordial stars in the local Universe.

ACKNOWLEDGEMENTS

JP thanks Roberto Gonzalez and Christian Wagner for their useful and constructive comments on this work. JP, RJ and LV acknowledge support by Mineco grant FPA2011-29678-C02-02. LV is supported by European Research Council under the European Communitys Seventh Framework Programme grant FP7- IDEAS-Phys.LSS.

REFERENCES

- Abel T., Bryan G. L. & Norman M. L., 2002, *Science*, 295, 93
- Barkana R. & Loeb A., 2001, *Phys. Rep.*, 349, 125
- Bougleoux E. & Galli D., 1997, *MNRAS*, 288, 638
- Bromm V., Coppi P. & Larson R. B., 2002, *ApJ*, 564, 23
- Bullock J. S., Kolatt T. S., Kravtsov A. V., Klypin A. A., Porciani C. & Primack J. R., 2001a, *ApJ*, 555, 240
- Davis A. J. & Natarajan P., 2009, *MNRAS*, 393, 1498
- Eisenstein D. J. & Hu W., 1998, *ApJ*, 496, 605
- Galli D. & Palla F., *P&SS*, 50, 1197
- Greif T. H., Johnson, Jarrett L., Klessen R. S. & Bromm, V., 2008, *MNRAS*, 387, 1021
- Greif T. H., Springel V., White S. D. M., Glover S. C. O., Clark P. C., Smith R. J., Klessen R. S. & Bromm V., 2011,
- Haiman Z., Thoul A. A. & Loeb A., 1996, *ApJ*, 464, 523
- Knollmann S. R. & Knebe A., 2009, *ApJ*, 182, 608
- Komatsu E., et al., 2009, *ApJS*, 180, 330
- Komatsu E., et al., 2010, *arXiv:1001.4538*
- Lepp S. & Shull J. M., 1983, *ApJ*, 270, 578
- Machida M., Tomisaka K., Nakamura F. & Fujimoto M., 2005, *ApJ*, 622, 39
- Palla F., Galli D. & Silk J., 1995, *ApJ*, 451, 401
- Peebles P. J. E., Dicke R. H., 1968, *ApJ* 154, 891
- arxiv.org/abs/1303.5076*
- Prieto J., Padoan P., Jimenez R., Infante L., 2011, *ApJ*, 731, L38
- Prieto J. P., Infante L., Jimenez R., 2008, *arXiv*, *arXiv:0809.2786*
- Prieto J., Jimenez R. & Martí J., 2012, *MNRAS*, 419, 3092P
- Prunet S. Pichon C., Aubert D., Pogosyan D., Teyssier R. & Gottloeber S., 2008, *ApJs*, 178, 179
- Tegmark M., Silk J., Rees M. J., Blanchard A., Abel T. & Palla F., 1997, *ApJ*, 474, 1
- Teyssier R., 2002, *A&A*, 385, 337
- Shchekinov Yu. A. & Vasiliev E. O., 2006, *MNRAS*, 368, 454
- Stacy A. & Bromm V., 2013, *MNRAS*, *arXiv:1211.1889*